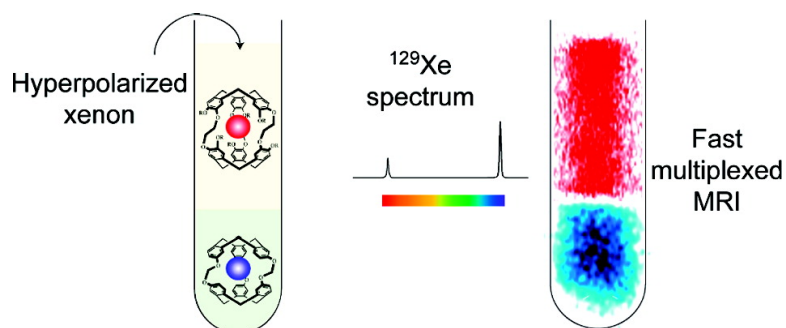


Sensitivity and Multiplexing Capabilities of MRI Based on Polarized Xe Biosensors

Patrick Berthault, Aurore Bogaert-Buchmann, Herve# Desvaux, Gaspard Huber, and Yves Boulard

J. Am. Chem. Soc., **2008**, 130 (49), 16456-16457 • DOI: 10.1021/ja805274u • Publication Date (Web): 14 November 2008

Downloaded from <http://pubs.acs.org> on February 8, 2009



More About This Article

Additional resources and features associated with this article are available within the HTML version:

- Supporting Information
- Access to high resolution figures
- Links to articles and content related to this article
- Copyright permission to reproduce figures and/or text from this article

[View the Full Text HTML](#)

Sensitivity and Multiplexing Capabilities of MRI Based on Polarized ^{129}Xe Biosensors

Patrick Berthault,^{‡,*} Aurore Bogaert-Buchmann,[‡] Hervé Desvaux,[‡] Gaspard Huber,[‡] and Yves Boulard[†]

CEA, IRAMIS, Service de Chimie Moléculaire, Laboratoire Structure et Dynamique par Résonance Magnétique, URA CEA/CNRS 331, 91191 Gif-sur-Yvette, France, and CEA, IBITECS, Service de Biologie Intégrative et Génétique Moléculaire, Laboratoire de Biologie Intégrative, 91191 Gif-sur-Yvette, France

Received July 8, 2008; E-mail: Patrick.Berthault@cea.fr

Hyperpolarized species, conceived with the aim of overcoming the low sensitivity of NMR and enabling early detection of biological events, are in constant development.¹ Recently a concept of molecular MRI has been proposed, where laser-polarized xenon is transported to the biological receptors of interest using functionalized host molecules.² The potential of this approach lies not only in the huge signal enhancement afforded by the optical pumping step but also in the possibility to refresh the system with hyperpolarized noble gas well after introduction of the host. Also, the chemically specific information of xenon in the hosts will enable spectroscopic imaging, owing to slow exchange conditions on the ^{129}Xe chemical shift time scale. Finally, simultaneous detection of correlated biological events should be possible through the use of different hosts bearing specific ligands, giving rise to distinct xenon peaks.^{2,3} This multiplexing capacity is assessed here with a simple MRI experiment, involving two cage molecules in two nonmiscible media. The execution of this experiment without any on-flow apparatus could give a representation of what could be encountered for *in vivo* experiments, where fast xenon longitudinal relaxation could impede the use of long experiments and render the attainment of very stable polarization illusory. Obviously, in this simplified system the xenon relaxation times are longer than those *in vivo*, and a delivery protocol-dependent extrapolation has to be performed.

Good candidates for the xenon biosensing approach are cryptophanes, cage molecules for which xenon exhibits high affinity and slow in–out exchange on the chemical shift time scale. Chemistry was developed to render the cryptophanes soluble in water,³ to graft tethers bearing specific ligands,^{4–6} or to build dendrimers designed to spatially concentrate the NMR signal.⁷ To date, the focus for xenon biosensors has been spectroscopic applications. No *in vivo* image has been reported, and the sensitivity requirement remains demanding.

We have prepared an NMR tube with the lower phase consisting of cryptophane-1.1.1 **C**₁, at a concentration of 300 μM in organic solvent **1**, and the upper phase consisting of water (solvent **2**) in which cryptophane-2.2.2 with carboxylate groups (compound **C**₂) is dissolved at a concentration of 300 μM (Figure 1). Both cryptophanes are known to encapsulate xenon, with binding constants at 293 K of 10 000 M^{-1} for the former⁸ and 6800 M^{-1} for the latter.³ At this temperature the characteristic times for xenon in–out exchange are ~ 100 and 10 ms, respectively. On the ^{129}Xe spectrum obtained with laser-polarized gas (Figure 1), four signals appear, corresponding to xenon in tetrachloroethane, xenon in water, xenon encapsulated in cryptophane **C**₂, and xenon encapsulated in cryptophane **C**₁, reading from low-field to high-field.

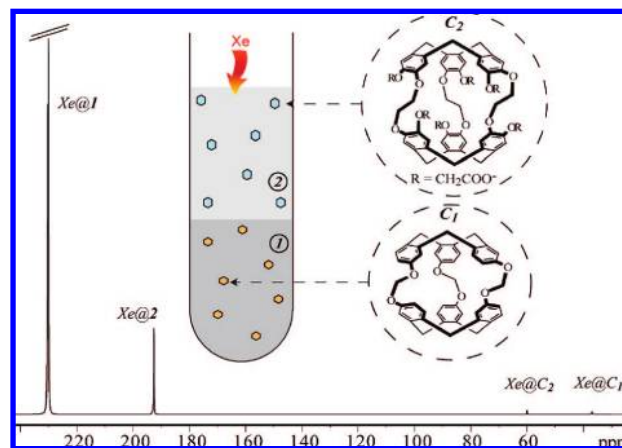


Figure 1. Studied system: the 8 mm tube (outer diameter) contains 200 μL $(\text{CHCl}_3)_2/(\text{CDCl}_3)_2$ (1:14) as lower phase, 300 μL $\text{H}_2\text{O}/\text{D}_2\text{O}$ (1:14) as upper phase, 43 μg of compound **C**₁, and 110 μg of **C**₂. ^{129}Xe spectrum obtained in one accumulation with ~ 1 atm of laser-polarized gas introduced on top of the solution (previously degassed).

For imaging the encapsulated noble gas, a fast gradient echo sequence is employed (Figure S1). It presents the advantage of possessing only one pulse per acquisition for a Cartesian sampling of the k reciprocal space. To allow frequency selection, the slice gradient during the excitation pulse is attenuated and the radio-frequency offset is centered on the $\text{Xe}@C_2$ frequency. For imaging $\text{Xe}@C_1$, the interleaved mode is used: a switch of the offset allows excitation of the resonance of xenon in the other cryptophane during the repetition time. The use of the centered phase encoding mode instead of a linear ramp of gradients enables one to take advantage of the highest polarization for defining the global shape of the object and to stop the acquisition at any moment according to the reservoir size of polarized spins (potentially at the price of a loss of spatial resolution in the phase dimension).

To fully take advantage of the in–out exchange behavior of xenon, the HYPERCEST approach⁹ was proposed: saturation at the $\text{Xe}@\text{host}$ frequency in one experiment and off-resonance in a second experiment enables by difference the identification of the biosensor through a change of the free Xe signal intensity. However, the validity of this approach first depends on the stability of the polarization level in solution, and second xenon diffusion is susceptible to lead to loss of spatial resolution and subtraction artifacts. Indeed, the average molecular displacement due to diffusion during the saturation delay is ~ 0.1 mm in the case of a closed system but can reach far higher values for *in vivo* applications due to the blood flow. Also, as the read pulse excites the free xenon signal, it is necessary to replenish the laser-polarized

[‡] CEA, IRAMIS.

[†] CEA, IBITECS.

xenon between two acquisitions or to use small flip angle read pulses. Thus we have preferred to resort to direct observation of the caged xenon signal. Possible broadening of the xenon peak due to transverse relaxation (the highest reported value is ~ 200 Hz for xenon in cryptophanes immobilized on agarose beads¹⁰) would only slightly reduce sensitivity in our approach (see Supporting Information).

Figure 2a and 2b show the images obtained with our system and pulse sequence. Each cryptophane in its compartment is perfectly localized, as can be seen by the separation at the water/organic solvent interface. No background noise appears in the other compartment. We are able to image in 25 s the noble gas in each of the cryptophanes of concentration $300 \mu\text{M}$ with a signal-to-noise ratio of 10 for $\text{Xe}@C_1$ and 6 for $\text{Xe}@C_2$ for a high planar resolution ($117 \times 125 \mu\text{m}^2$). Assuming that all the cages are occupied by the noble gas, this would roughly correspond to the detection of 10^{13} spins per voxel.

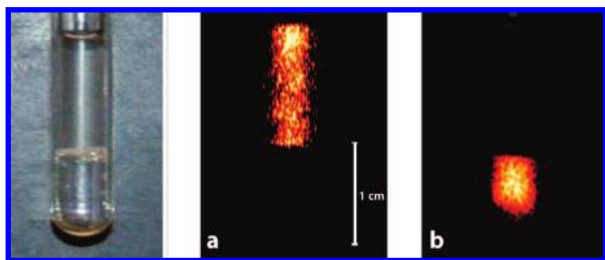


Figure 2. ^{129}Xe images of xenon caged in (a) cryptophane C_2 (in D_2O) and in (b) cryptophane C_1 (in $(\text{CDCl}_2)_2$). No slice selection is used. The number of points is 128 in the read dimension (axis of the tube) and 64 in the phase dimension. No zero-filling is applied before Fourier transformation.

The xenon hyperpolarization is not completely destroyed by the MRI pulse sequence, and spectra with a good signal-to-noise ratio in one accumulation could be obtained after the images, proving that the image resolution and/or signal-to-noise ratio can even be increased. Such images could be recorded several times with a good contrast after shaking the tube. As time passes, only the signal of xenon in C_1 remains. This can be explained by the bigger reservoir of laser-polarized xenon atoms around the C_1 cage due to the larger xenon solubility in **1** compared with **2**. In the gradient echo experiment, slice selection is possible by combining a highly selective soft pulse and low gradient strength (Figure S2). Also, more sophisticated detection schemes based for instance on Echo Planar Imaging could be employed, but would be more prone to artifacts due to motions and magnetic susceptibility variations.

Obviously, biosensor concentrations on the order of $100 \mu\text{M}$ are still too high for realistic *in vivo* molecular imaging applications when compared to cell receptor concentrations, but in these experiments, the requirements of spatial resolution are far less stringent: an increase of pixel size for instance by a factor of 70

would maintain a millimeter resolution while allowing reduction of the xenon host concentration by the same factor. Also, as exploited by Schröder et al.¹¹ the optimization of in-out exchange rate can guarantee the success of these experiments. Finally, for *in vivo* applications, slowing down the apparent decay of dissolved xenon polarization, i.e., by resorting to new gas bolus or optimized xenon carriers, would also allow a decrease of xenon host concentration. The main limiting parameter is the relaxation time of free dissolved xenon: using another NMR tube prepared with C_1 at a concentration of $25 \mu\text{M}$ in solvent **1**, with the same pulse sequence assuring that we only observe caged xenon, we have obtained an image with a signal-to-noise ratio of 5 and a resolution of $117 \times 250 \mu\text{m}^2$ in 204 s (Figure S3).

The gradient-echo sequence described here offers the advantage of both simplicity and rapidity. The experiment has shown that simultaneous discrimination via the chemical shifts of xenon in two different cages is possible and confirmed that the image corresponds well to caged xenon and is not due to a residual of rf irradiation at the $\text{Xe}@$ solvent frequency.

Acknowledgment. The authors thank Drs. H. A. Fogarty, J.-P. Dutasta, and T. Brotin from ENS Lyon for providing the two cryptophanes and Dr. A. Yuen for careful reading of the manuscript. Financial support from the Conseil Général de l'Essonne (ASTRE 2003 program) and from the French Ministry of Research (ANR program "Physico-Chimie du Vivant 2006") is greatly acknowledged.

Supporting Information Available: Experimental details for the preparation of laser-polarized xenon, NMR and MRI sequences, images obtained with slice selection and at $25 \mu\text{M}$ cryptophane. This material is available free of charge via the Internet at <http://pubs.acs.org>.

References

- (1) Golman, K.; in't Zandt, R.; Thaning, M. *Proc. Natl. Acad. Sci. U.S.A.* **2006**, *103*, 11270.
- (2) Spence, M. M.; Rubin, S. M.; Dimitrov, I. E.; Ruiz, E. J.; Wemmer, D. E.; Pines, A.; Qin Yao, S.; Tian, F.; Schultz, P. G. *Proc. Natl. Acad. Sci. U.S.A.* **2001**, *98*, 10654.
- (3) Huber, G.; Brotin, T.; Dubois, L.; Desvaux, H.; Dutasta, J.-P.; Berthault, P. *J. Am. Chem. Soc.* **2006**, *128*, 6239.
- (4) Lowery, T. J.; Garcia, S.; Chavez, L.; Ruiz, E. J.; Wu, T.; Brotin, T.; Dutasta, J.-P.; King, D. S.; Schultz, P. G.; Pines, A.; Wemmer, D. E. *ChemBioChem* **2006**, *7*, 65.
- (5) Wei, Q.; Seward, G. K.; Hill, P. A.; Patton, B.; Dimitrov, I. E.; Kuzma, N. N.; Dmochowski, I. J. *J. Am. Chem. Soc.* **2006**, *128*, 13274.
- (6) Roy, V.; Brotin, T.; Dutasta, J.-P.; Charles, M.-H.; Delair, T.; Mallet, F.; Huber, G.; Desvaux, H.; Boulard, Y.; Berthault, P. *ChemPhysChem* **2007**, *8*, 2082.
- (7) Mynar, J. L.; Lowery, T. J.; Wemmer, D. E.; Pines, A.; Frechet, J. M. J. *J. Am. Chem. Soc.* **2006**, *128*, 6334.
- (8) Fogarty, H. A.; Berthault, P.; Brotin, T.; Huber, G.; Desvaux, H.; Dutasta, J.-P. *J. Am. Chem. Soc.* **2007**, *129*, 10332.
- (9) Schröder, L.; Lowery, T. J.; Hilty, C.; Wemmer, D. E.; Pines, A. *Science* **2006**, *314*, 446.
- (10) Hilty, C.; Lowery, T. J.; Wemmer, D. E.; Pines, A. *Angew. Chem. Int. Ed.* **2006**, *45*, 70.
- (11) Schröder, L.; Chavez, L.; Meldrum, T.; Smith, M.; Lowery, T. J.; Wemmer, D. E.; Pines, A. *Angew. Chem., Int. Ed.* **2008**, *47*, 4316.

JA805274U